Supplemental Material

MRI of mouse cerebral cavernomas reveal differential lesion progression and variable permeability to gadolinium

Delaney G. Fisher[1,#], Khadijeh A. Sharifi[2,3,#], E. Zeynep Ulutas[4], Jeyan S. Kumar[3], M. Yashar S. Kalani[5], G. Wilson Miller[1,6], Richard J. Price[1], Petr Tvrdik[2,3]

1. Department of Biomedical Engineering, University of Virginia, Charlottesville, VA
2. Department of Neuroscience, University of Virginia, Charlottesville, VA
3. Department of Neurosurgery, University of Virginia Health System, Charlottesville, VA
4. Department of Neuroscience, Georgia Institute of Technology, Atlanta, GA
5. St. John's Neuroscience Institute, Tulsa, OK
6. Department of Radiology & Medical Imaging, University of Virginia, Charlottesville, VA

[#]Authors contributed equally

Correspondence:

Petr Tvrdik, Ph.D.
409 Lane Road, MR-4, Room 1011,
Charlottesville, VA 22908.
Phone: 434-924-1956
Email: tvrdik@virginia.edu

Figure S1

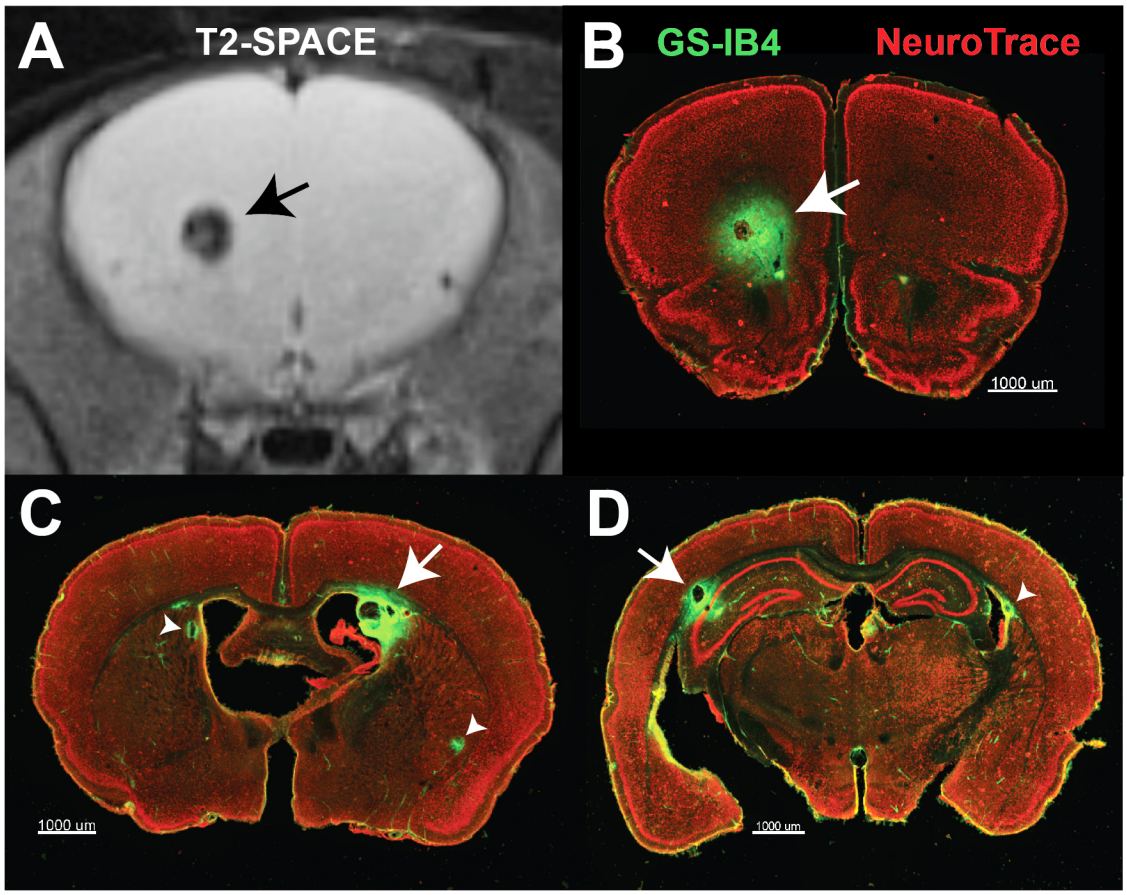

Figure S1. The anatomical distribution of vascular lesions in the *Krit1* CCM model. **A-B**, Alignment of a T2-SPACE MRI image plane with the corresponding brain section labeled with fluorescent isolectin GS-IB4 (green) and Neuro-Trace Nissl stain (red; n=1). **C**, In this mouse model, cavernous lesions frequently occur in dorsal striatum near lateral ventricles (white arrow). **D**, CCM lesions are also commonly found in the subcortical white matter of the corpus callosum, often adjacent to the dorsal hippocampus. (white arrow, arrow head). This Figure S1 is related to Figure 1.

Figure S2

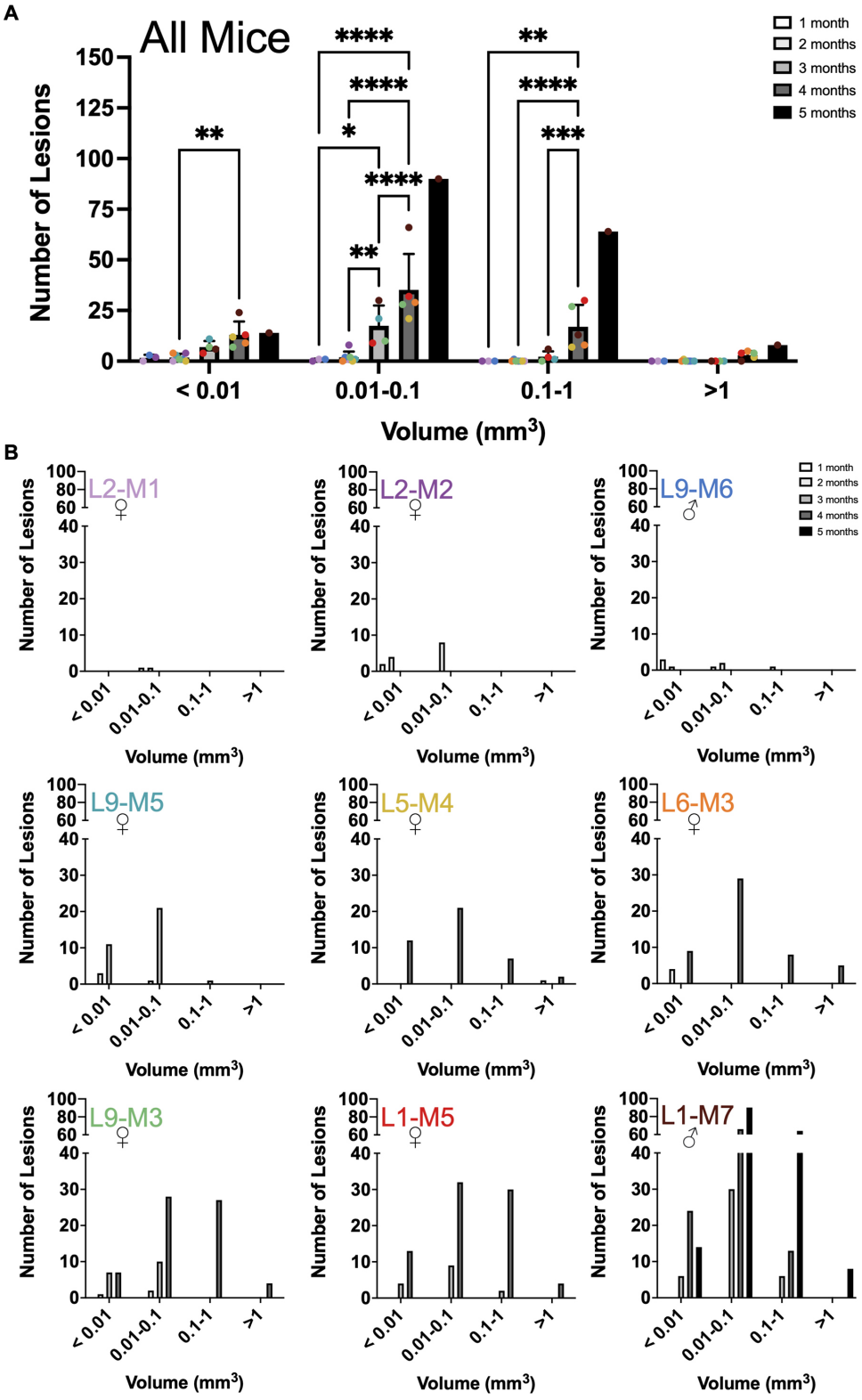

Figure S2. Number of small, intermediate, and large cerebral lesions at different age points in the *Krit1* CCM model. A, Lesion sizes were binned into 4 size groups V1-V4 (V1<0.01 mm^3;

Figure S2

0.01 $mm^3 \leq V2 < 0.1\ mm^3$; $0.1\ mm^3 \leq V3 < 1\ mm^3$; and $V4 \geq 1\ mm^3$). The number of lesions in each size group is plotted for each age point in the cohort (19 measurements in 9 mice). **B**, Total number of lesions in each size bin and imaging time point is plotted for every animal individually. Graph titles indicate unique mouse ID where L# denotes litter number and M# denotes arbitrary mouse number within litter. Sex of mice is indicated with the symbol ♀ for females (n=7) and ♂ for males (n=2). *, $p \leq 0.05$; **, $p \leq 0.01$; ***, $p \leq 0.001$; ****, $p \leq 0.0001$; mixed-effects model with repeated measures and Tukey's multiple comparisons test on datasets with $n \geq 3$. This Figure S2 is related to Figure 2.

Figure S3

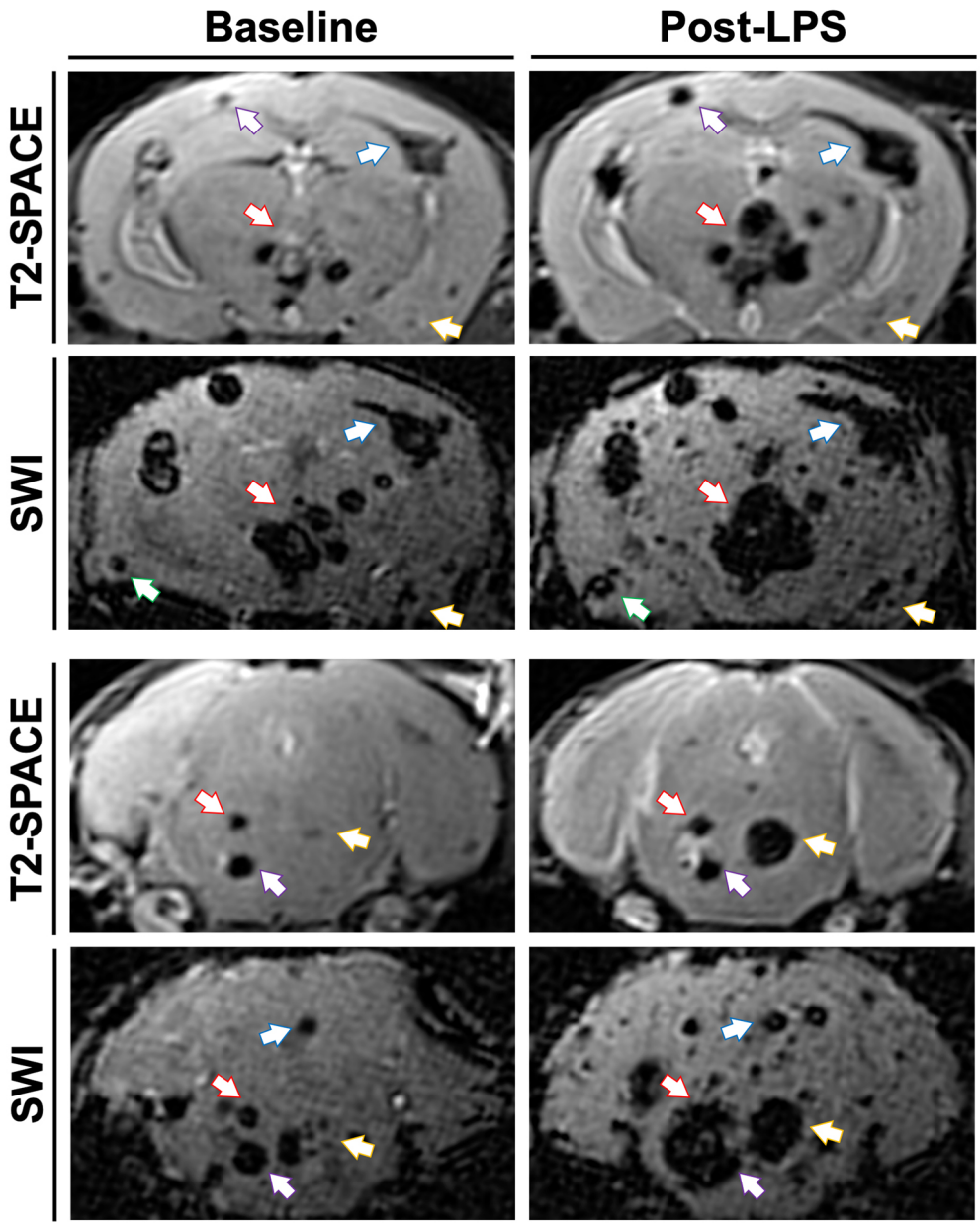

Figure S3. Comparison of T2-SPACE and SWI sequence sensitivity before and after a sudden hemorrhagic episode. The *Pdgfb-CreERT*; *Krit1* $^{fl/null}$ mouse (n=1) was imaged at Baseline and 12 h after acute mild neuroinflammation induced with LPS (0.25 mg/kg i.p.). Matching coronal planes of T2-SPACE and SWI are shown, demonstrating increased SWI sensitivity to CCM lesions. However, the exaggerated distortion of the lesion size is also apparent. Note the substantial increase in lesion volumes following neuroinflammation, accelerated due to fatal bleeding. Arrows identify the corresponding lesions between MRI sequences and inflammatory states.

Figure S4

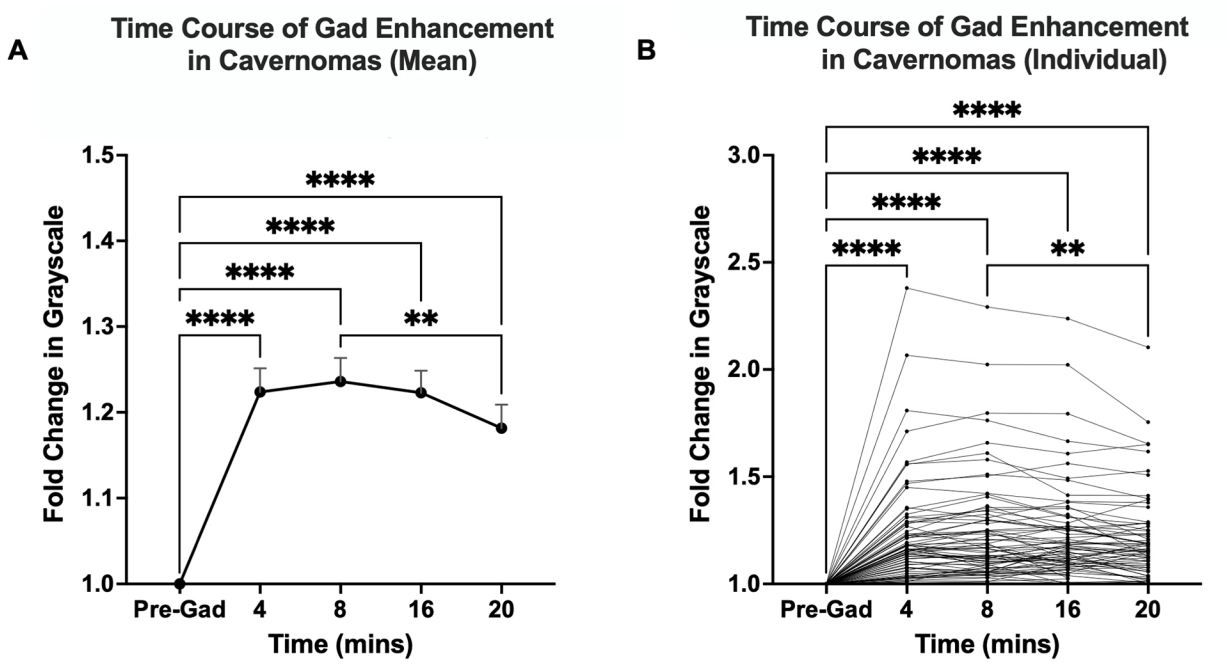

Figure S4. Time course of T1 gadolinium-contrast enhancement within cavernomas in the L1-M7 animal (n=1). **A-B**, Line graphs displaying fold change in grayscale intensity of 74 cavernomas at various times following gadolinium intravenous injection over pre-gadolinium T1-weighted image. **A**, Average fold change in grayscale intensity value for the 74 cavernomas. **B**, Individual fold change in grayscale intensity values for the 74 cavernomas. T1 contrast enhancement significantly increased from the pre-gadolinium image to 4 minutes post injection and significantly decreased at 20 minutes post injection. No statistically significant differences were found between the measurements obtained at 4 mins, 8 mins, or 16 mins post injection. **, $p \leq 0.01$; ****, $p \leq 0.0001$; One-way repeated measures ANOVA with Tukey's multiple comparisons test. This Figure S4 is related to Figure 3.

Figure S5

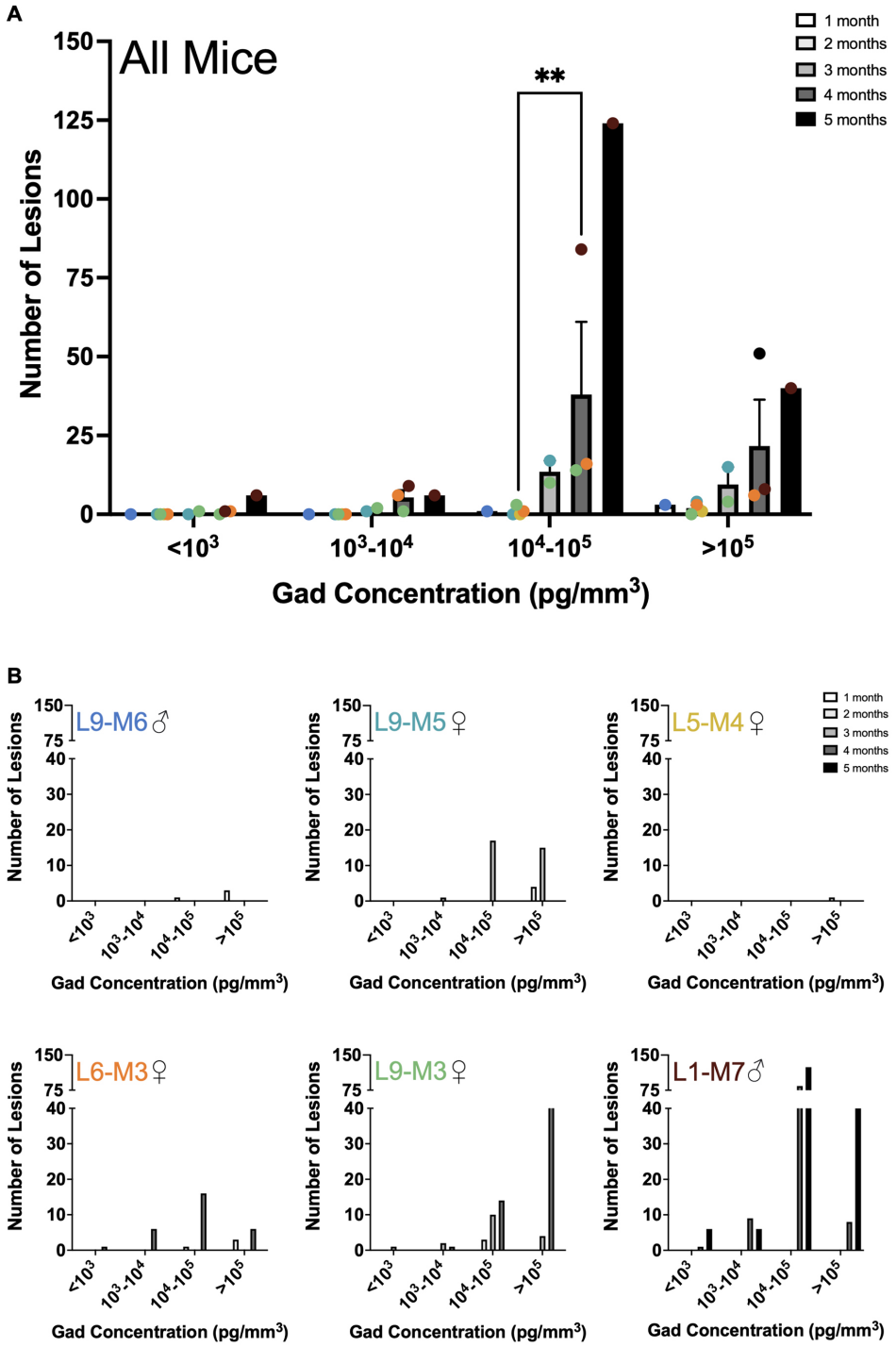

Figure S5. Number of lesions with low, medium, and high permeability at different age points in the *Krit1* CCM model. A, The lesions were binned by four gadolinium concentration levels G1-G4 ($G1<10^3$ pg/mm^3; 10^3 pg/mm^3$\leq G2<10^4$ pg/mm^3; 10^4 pg/mm^3$\leq G3<10^5$ pg/mm^3; and $G4\geq10^5$ pg/mm^3). The number of lesions in each permeability bin and each age-point is plotted for the whole cohort (11 measurements in 6 mice). **B**, Total number of lesions for each gadolinium concentration range and imaging time point is plotted for each animal individually. Graph titles

Figure S5

indicate unique mouse ID where L# denotes litter number and M# denotes arbitrary mouse number within litter. Sex of mice is indicated with the symbol ♀ for females (n=4) and ♂ for males (n=2). **, p≤0.01; mixed-effects model with repeated measures and Tukey's multiple comparisons test on datasets with n≥3. This Figure S5 is related to Figure 3.

Figure S6

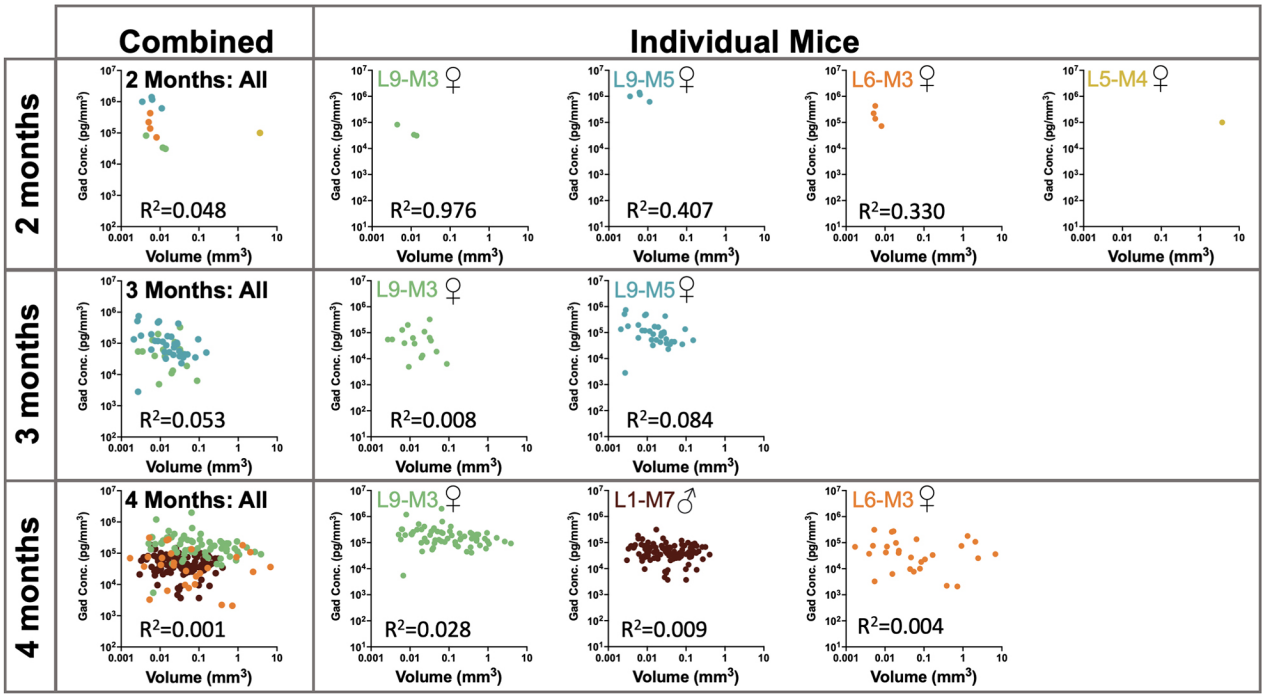

Figure S6. Lesion permeability is poorly correlated with lesion volume. Log-log graphs of gadolinium concentration as a function of lesion volume for individual lesions at each imaging time point. Data for all mice (n=5) at 2 months, 3 months, and 4 months is shown on the left. Data for individual mice and corresponding coefficients of determination values are disaggregated on the right. The coefficients of determination (R^2) indicate poor correlation between gadolinium concentration and volume at all time points, suggesting highly heterogenous permeability of lesions across age in this CCM model. Sex of mice is indicated with the symbol ♀ for females (n=4) and ♂ for males (n=1).

Figure S7

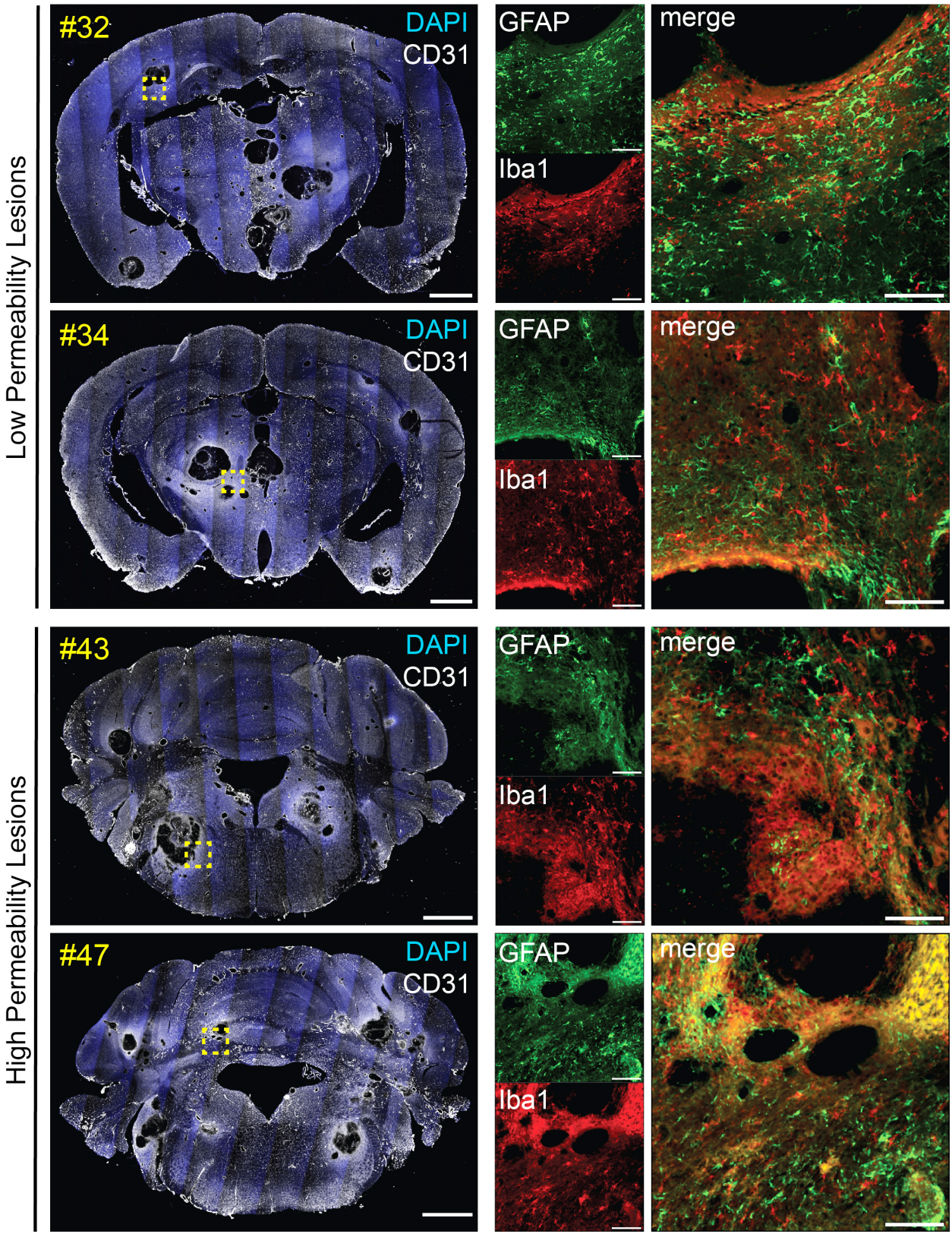

Figure S7. Anatomical and cellular context of CCM lesions with low and high permeability in L9-M3 (n=1). On the left: Tiled confocal images of brain coronal sections harboring the lesions

Figure S7

with the lowest permeability (#32 in the subcortical corpus callosum and #34 in the thalamus, see Supplemental Table S3 for an overview of measurements) are shown on top. Two lesions with the highest permeability (#43 in the brainstem and #47 in the cerebellum, see Supplemental Table 1 for detail) are shown at the bottom. The tiled coronal sections, scanned at a low resolution, show the overlay of nuclear stain DAPI (blue) and CD31 endothelial cell marker (white). The area marked with the yellow dashed box in each coronal section was imaged at a higher resolution, and the corresponding images of GFAP-positive astrocytes (green) and Iba1-positive microglia/macrophages (red), as well as the merged overlay, are shown on the right. The lesions with a high gadolinium content appear to have fewer glial cells in the immediate vicinity of the borders. Scale bars: tiled coronal section images, 1 mm; high-resolution IHC panels, 100 μm. This Figure S7 is related to Figure 5.

Figure S8

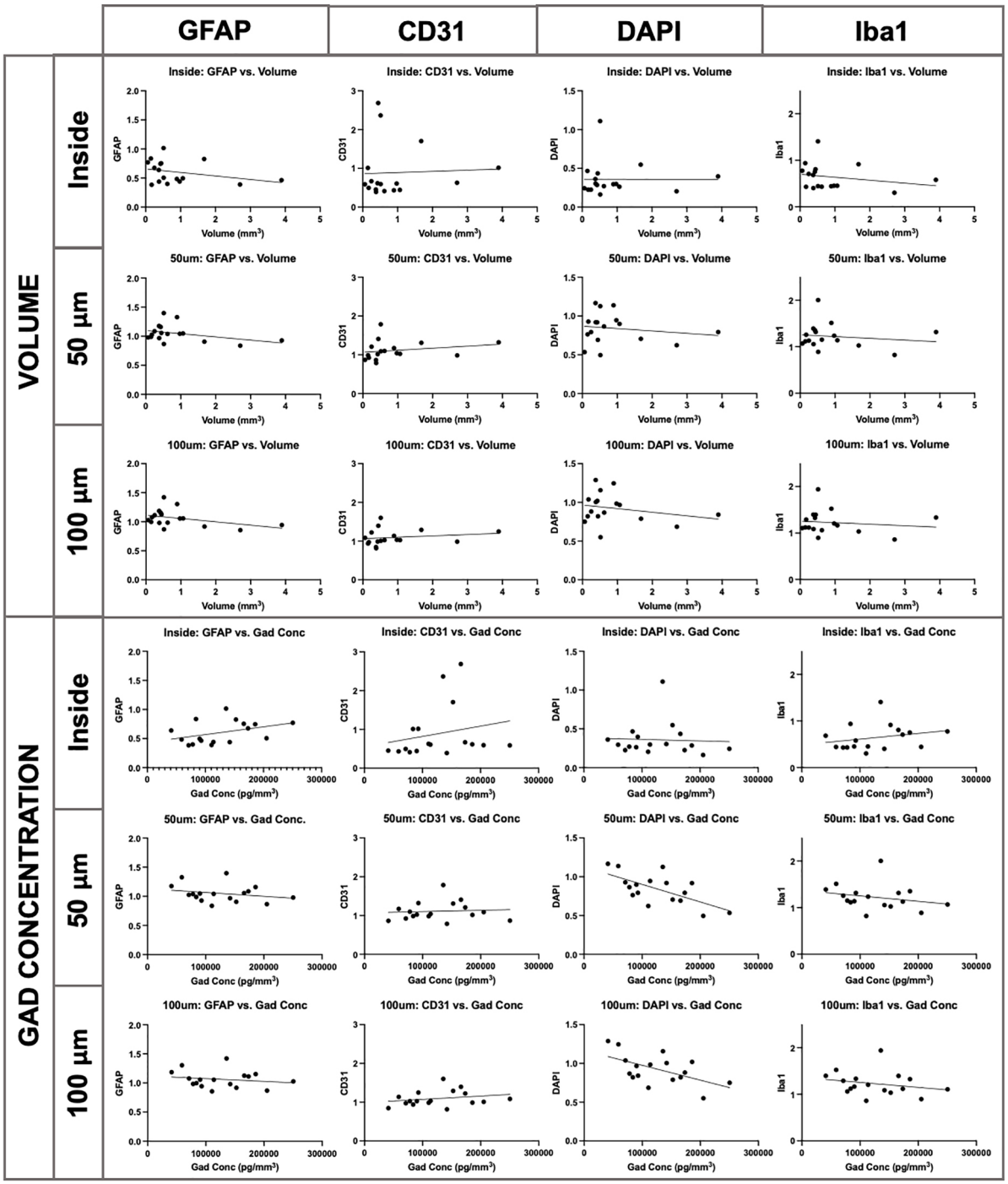

Figure S8. Correlations between MR signatures and IHC signatures in L9-M3 (n=1). Correlation plots for individual cell populations (astrocytes-GFAP, endothelial cells-CD31, cell nuclei-DAPI, and microglia-Iba1) and MR features (lesion volume and lesion permeability) at different locations around the lesion (inside lesion, 50µm border outside lesion, and 100µm border outside lesion). Dots indicate the 17 individual lesions. Linear regression fitted to each dataset.

Figure S9

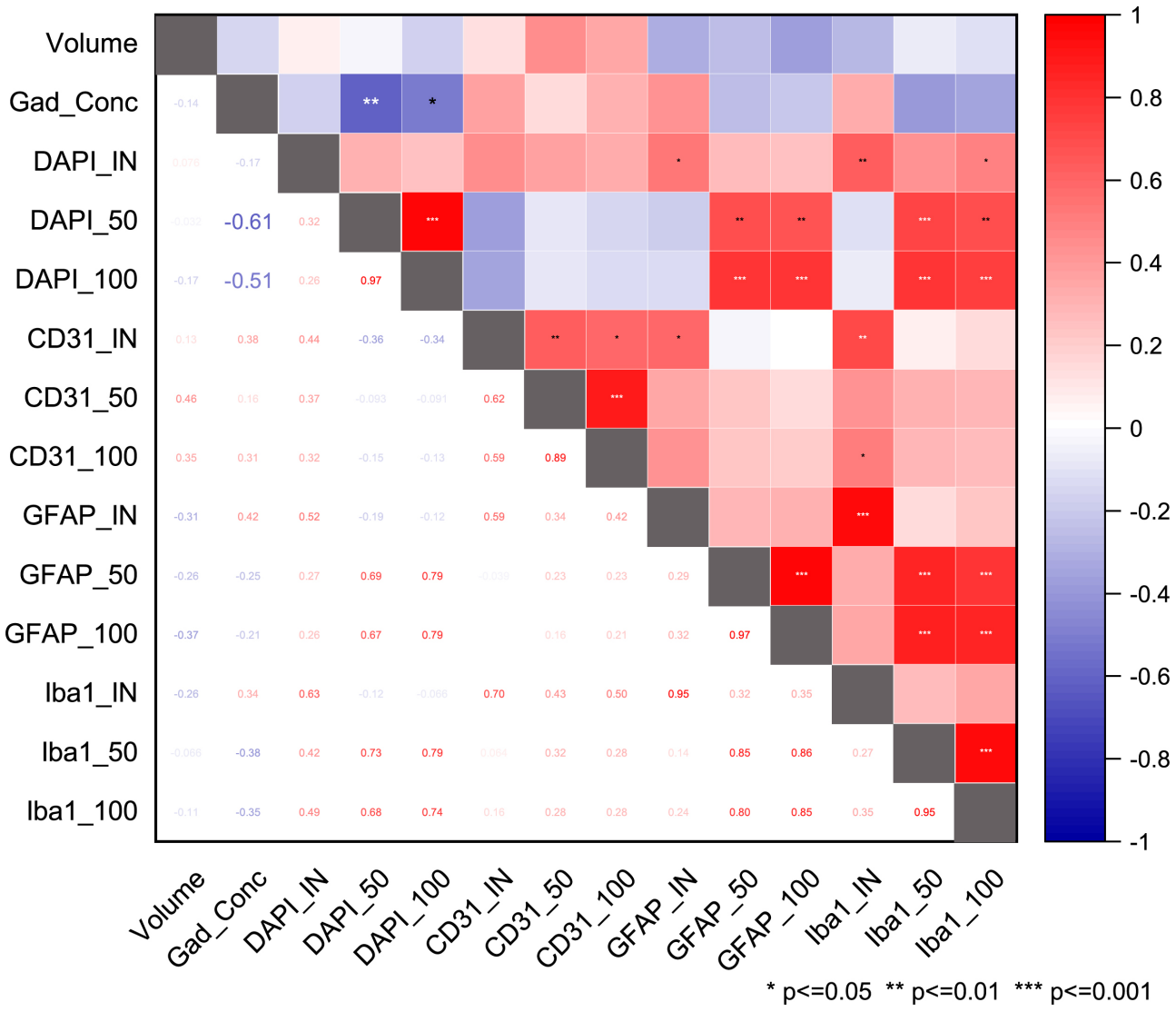

Figure S9. Correlation Matrix Heatplot of 14 variables in 17 different CCM lesions in the L9-M3 animal (n=1). Two variables, Volume and Gad Concentration, were measured with MRI, the values of the remaining 12 variables were obtained with confocal image analysis of brain sections stained with IHC inside the lesions, as well as in 50- and 100-µm perimeters outside the lesions. Significant inverse correlations between MRI and IHC were found for gadolinium concentration and DAPI intensity for both 50-µm and 100-µm border perimeters (r = - 0.61, p = 0.009; and r = - 0.51, p = 0.036; respectively). The plot was generated with OriginPro 2020.

Figure S10

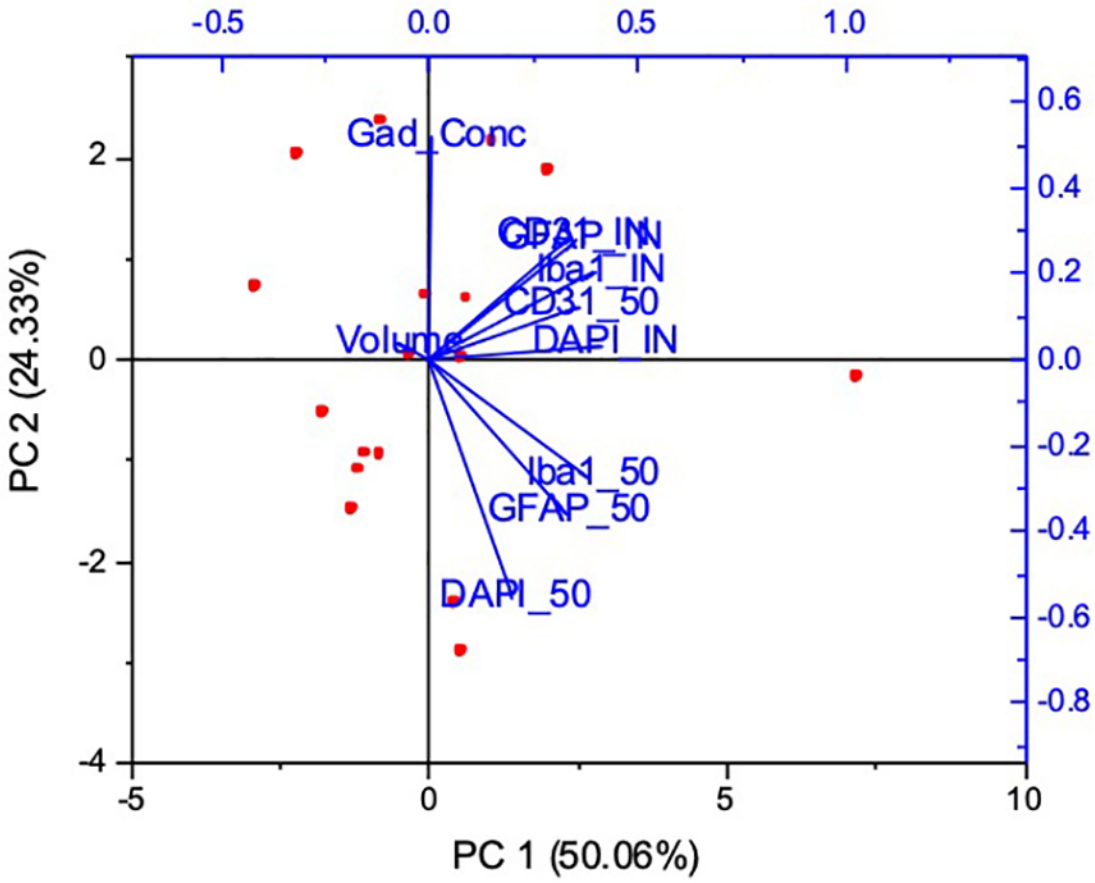

Figure S10. Principal component analysis (PCA) of 10 variables in 17 different CCM lesions in the L9-M3 animal (n=1). The plot includes volume and gadolinium concentration (Gad_Conc), as well as the IHC values inside the lesions (DAPI, GFAP, Iba1, CD31). Only the 50-µm perimeters were included in this analysis for the sake of clarity. PCA analysis corroborates the inverse correlation of gadolinium concentration and DAPI intensity outside the lesions, and reveals trends towards inverse correlation between gadolinium concentration and Iba1 and GFAP fluorescence intensity outside the lesions. The plot was generated with OriginPro 2020.

Legends for Supplemental Videos

Video S1

Longitudinal T2-SPACE MR images demonstrate an increase in lesion load with age. Movie of T2-SPACE images of mouse L1-M7 from timepoints of 3 months, 4 months, and 5 months of age. Lesions are denoted with manually drawn ROIs in each MR slice. Lesion burden is seen to increase with age.

Video S2

MR images of T2-SPACE and gadolinium concentration maps indicated variability of individual lesion permeability. Animations include T2-SPACE MR images, gadolinium concentration maps, and merged images of mouse L1-M7 at 5 months of age.

Video S3

Longitudinal MR images of merged T2-SPACE and gadolinium concentration maps indicate an increase in cumulative lesion permeability with age. Movies consist of merged T2-SPACE images and gadolinium concentration maps of mouse L1-M7 from timepoints of 4 months and 5 months of age. Overall lesion permeability is seen to increase with age.

Supplemental Tables

Table S1. Random coefficient regression analysis of total lesion volumes in Figure 2B

Table S1a. Summary statistics for Total Lesion Volume (mm^3), stratified by mouse age.

Month	n	Mean	Standard Deviation	Standard Error	Geom. Mean	Median	Interquartile Range		Minimum	Maximum
1	3	0.03	0.02	0.01	0.03	0.04	0.03	0.04	0.02	0.05
2	7	0.62	1.35	0.51	0.11	0.04	0.03	0.28	0.02	3.68
3	4	0.95	0.73	0.37	0.78	0.71	0.51	1.15	0.37	2.01
4	5	28.56	30.04	13.43	19.78	18.49	15.45	21.52	6.07	81.29
5	1	46.72			46.72	46.72	46.72	46.72	46.72	46.72

Table S1b. Intercept and slope coefficients for the random coefficient regression of $\log_{10}$(Total Lesion Volume [mm^3]) onto mouse age.

Parameter	Estimate	Standard Error	Lower 95% CL	Upper 95% CL	t-statistics	P-value
Intercept	-2.790	0.335	-3.496	-2.084		
Slope	0.976	0.111	0.742	1.211	8.762	<0.001

Logarithmic base 10 Scale - Marginal Random Coefficient Regression Equation:

$$E(\log_{10}(\text{Total Lesion Volume } [mm^3])|\text{Age}) = -2.790 + 0.976 \times \text{age}.$$

Original Scale - Marginal Random Coefficient Regression Equation:

$$E(\text{Total Lesion Volume } [mm^3]|\text{Age}) = 0.0016 \times 10^{[0.976 \times \text{Age}]}$$

Table S2. Random coefficient regression analysis of total gadolinium permeability in Figure 3B

Table S2a. Summary statistics for Total Lesion Gad Mass (pg), stratified by mouse age.

Month	n	Mean	Standard Deviation	Standard Error	Geom. Mean	Median	Interquartile Range		Minimum	Maximum
1	1	475654			475654	475654	475654	475654	475654	475654
2	4	1323047	1938784	969392	479920	504084	135385	1691746	100068	4183952
3	2	3084525	2698345	1908018	2423584	3084525	2130516	4038534	1176507	4992543
4	3	7517977	6732847	3887211	5517069	5483267	3760215	10258380	2037163	15033500
5	1	12500000			12500000	12500000	12500000	12500000	12500000	12500000

Table S2b. Intercept and slope coefficients for the random coefficient regression of $\log_{10}$(Total Lesion Gad Mass [pg]) onto mouse age.

Parameter	Estimate	Standard Error	Lower 95% CL	Upper 95% CL	t-statistics	P-value
Intercept	4.971	0.371	4.093	5.848		
Slope	0.398	0.089	0.180	0.617	4.488	0.004

Logarithmic base 10 Scale - Marginal Random Coefficient Regression Equation:

$$E(\log_{10}(\text{Total Lesion Volume } [mm^3])|\text{Age}) = 4.971 + 0.398 \times \text{age}.$$

Original Scale - Marginal Random Coefficient Regression Equation:

$$E(\text{Total Lesion Gad Mass [pg]}|\text{Age}) = 93510.57 \times 10^{[0..398 \times \text{Age}}$$

Table S3. MRI and IHC data on 17 lesions obtained from animal L9-M3.

			Inside Mean (Reps Avg)				100um Mean (Reps Avg)				50um Mean (Reps Avg)			
Lesion	Gad Conc (pg/mm^3)	Volume (mm^3)	GFAP_inside	CD31_inside	DAPI_inside	Iba1_inside	GFAP_100un	CD31_100un	DAPI_100um	Iba1_100um	GFAP_50um	CD31_50um	DAPI_50um	Iba1_50um
12	92714.5788	3.8942	0.46431863	1.01534338	0.39739129	0.58003318	0.94344428	1.24834218	0.84130118	1.33337894	0.92819999	1.32170925	0.79301331	1.31549563
16	113740.0996	0.9725	0.44099493	0.60750498	0.29784429	0.45337761	1.05657798	1.03322419	0.98448816	1.2047426	1.04330989	1.04137755	0.94552601	1.2354617
17	110661.7079	2.7031	0.38937866	0.62818661	0.2048617	0.30379374	0.8551767	0.98707081	0.68545834	0.86080886	0.83671356	0.98295539	0.62263874	0.82109026
18	152649.9725	1.6776	0.82669582	1.70259179	0.54788267	0.91609303	0.91692457	1.29233802	0.78997916	1.03453302	0.90555817	1.30880106	0.70567011	1.02616352
19	135598.183	0.5125	1.01641016	2.36726778	1.10923653	1.40645212	1.4206322	1.60233765	1.15720102	1.93994806	1.39806536	1.78651591	1.12710486	2.00208622
20	90145.63991	1.0659	0.49600156	0.44496801	0.26312907	0.45317014	1.05704584	1.02678042	0.96732064	1.16566499	1.04721102	1.0239466	0.89858737	1.13835663
30	78085.07867	0.6213	0.39885241	0.41496721	0.27075706	0.43231426	0.98397994	1.02685786	0.86826289	1.06163354	1.03980435	1.09825813	0.86581851	1.1515327
31	71134.76341	0.1706	0.38462935	0.49633306	0.22619912	0.43015429	1.07708834	0.9729577	1.03793697	1.29016273	1.02532204	0.92479411	0.92802168	1.25638964
32	41019.87042	0.3754	0.6389012	0.45388075	0.36212609	0.68347586	1.18503577	0.84585389	1.28792896	1.39640469	1.17517655	0.86468505	1.16644144	1.3908819
33	141878.8492	0.3832	0.43839389	0.39165771	0.30476375	0.40286051	0.98028225	0.81571769	1.00408845	1.08561283	0.96757882	0.78639576	0.91928778	1.05418382
34	58894.88952	0.894	0.48341992	0.43373104	0.29580202	0.44306105	1.30477273	1.1364358	1.24621049	1.52406022	1.32721962	1.1706922	1.13792745	1.51234684
43	185812.8089	0.424	0.74515852	0.61632318	0.2855843	0.75269869	1.15277551	0.98880473	1.01938653	1.32610403	1.15967395	1.01563284	0.91807499	1.3538739
44	166056.7799	0.442	0.75415504	2.68520111	0.43552906	0.80703634	1.12553339	1.39724704	0.82082223	1.39513438	1.05623473	1.40830901	0.69221363	1.31614934
45	83752.36809	0.1478	0.83629065	1.01151024	0.46652356	0.93781281	0.99701947	0.93919582	0.82031542	1.12239723	0.98945611	0.98743172	0.76259297	1.11489603
46	205300.9457	0.5158	0.50572214	0.5932727	0.16259457	0.44456393	0.86956832	1.00766763	0.55031929	0.89620943	0.86603	1.08794183	0.49567473	0.88856042
47	250453.6696	0.0632	0.77136785	0.58877769	0.24307874	0.77660994	1.02736035	1.08461039	0.75109719	1.10625199	0.97977754	0.86874446	0.53468568	1.06765946
50	173442.2976	0.2495	0.67587646	0.6675078	0.22576538	0.70773858	1.11266199	1.22339701	0.88156548	1.11725933	1.08566037	1.20825458	0.79274544	1.12942283

Major Resources Table

Animals (in vivo studies)

Species	Vendor or Source	Background Strain	Sex	Persistent ID / URL
Mice	The Jackson Laboratory	C57BL/6J	both	Strain #:000664 RRID:IMSR_JAX:000664

Genetically Modified Animals

	Species	Vendor or Source	Background Strain	Persistent ID / URL
Pdgfb-iCreERT2-IRES-EGFP	Mice	Dr. Kevin Whitehead lab, University of Utah	C57BL/6J; 129/Sv	DOI: 10.1002/dvg.20367
Krit1 flox/null	Mice	Dr. Kevin Whitehead lab, University of Utah	C57BL/6J; 129/Sv	DOI: 10.1002/dvg.20367

Antibodies

Target antigen	Vendor or Source	Catalog #	Working conc.	Persistent ID / URL
Chicken anti-GFAP	Aves Labs	GFAP	(1:200)	RRID: AB_2313547
Rabbit anti-Iba1	Wako Chemicals USA	016-20001	(1:500)	RRID:AB_839506
Goat anti-CD31	R&D Systems	AF3628	(1:20)	RRID:AB_2161028
Donkey anti-chicken Alexa 488	Jackson ImmunoRes. Labs	703-546-155	(1:500)	RRID:AB_2340376
Donkey anti-rabbit Alexa 568	Invitrogen	A10042	(1:500)	RRID:AB_2534017
Donkey anti-goat Alexa 647	Invitrogen	A21447	(1:500)	RRID:AB_2535864

Data & Code Availability

Description	Source / Repository	Persistent ID / URL
MRI DICOM files	UVA Libra	https://www.library.virginia.edu/libra

Other

Description	Source / Repository	Persistent ID / URL
NeuroTrace™ 530/615 Red Fluorescent Nissl Stain	Invitrogen	N21482; RRID: AB_2620170
Isolectin GS-IB_4 From *Griffonia simplicifolia*, Alexa Fluor™ 488 Conjugate	Invitrogen	I21411; RRID: AB_2314662
Fluoromount-G	SouthernBiotech	0100-01
Fluoromount-G™ Mounting Medium, with DAPI	Invitrogen	Cat# 00-4959-52 Lot No. E141818
DAPI	ThermoFisher	D1306
PBS (Phosphate-Buffered Saline)	Sigma-Aldrich	P4417-100 TAB
Sucrose	Sigma Millipore	S1888-500G
32% Paraformaldehyde aqueous solution	EMS	50-980-495
Triton X-100	Sigma-Aldrich	T8787-100 ml
Bovine serum albumin (BSA)	Jackson ImmunoResearch Labs	001-000-161; RRID: AB_2336945
Normal donkey serum (NDS)	Jackson ImmunoResearch Labs	017-000-121 RRID: AB_2337258
Tissue-Tek O.C.T. Compound	Andwin Scientific	4583
Secure Seal Spacers	EMS	70327-20S
Microscope slides	FisherScientific	12-5550-15
Fisherbrand Microscope Cover Glass	FisherScientific	12544E
Corn oil	Sigma-Aldrich	C8267-500 mL

DOI [to be added]

Tamoxifen	Sigma-Aldrich	T5648-5G
lipo-polysaccharides (LPS)	Sigma-Aldrich	L4391
Isoflurane	Dechra	17033-094-25
MultiHance (gadobenate dimeglumine)	Bracco	0270-5164-15; 20mL vials

ARRIVE GUIDELINES

The ARRIVE guidelines (https://arriveguidelines.org/) are a checklist of recommendations to improve the reporting of research involving animals. Key elements of the study design should be included below to better enable readers to scrutinize the research adequately, evaluate its methodological rigor, and reproduce the methods or findings.

Study Design

Groups	Sex	Age	Number (prior to experiment)	Number (after termination)	Littermates (Yes/No)	Other description
Pdgfb-CreERT2; Krit1 flox/null	M & F	1-5 m	35	9 (2M & 7F)	yes	MRI, histology
Pdgfb-CreERT2; Krit1 flox/wt	M & F	1-5 m	4	4 (2M & 2F)	yes	neg. control
Krit1 flox/null	M & F	1-5 m	4	4 (2M & 2F)	yes	neg. control

Sample Size: The study was designed as an exploratory study and formal sample size calculation was not performed.

Inclusion Criteria: *Pdgfb-CreERT2; Krit1 flox/null* genotype, two or more MRI scans spaced by 1 month available

Exclusion Criteria: Stunted growth, lethargic behavior, hunched posture and visible skin wounds, unusually low body weight.

Randomization: Not applicable; mice were assigned to groups according to their genotype, sex and age

Blinding: Yes

DOI [to be added]